Supporting information

C_3N_4-digested 3D construction of hierarchical metallic phase MoS_2 nanostructures

Jiayu Wang[1], Jing Tang[2*], Tong Guo[1], Shuaihua Zhang[3,4], Wei Xia[3], Haibo Tan[3], Yoshio Bando[3], Xin Wang[1*] and Yusuke Yamauchi[5*]

1. Key Laboratory for Soft Chemistry and Functional Materials of Ministry Education, Nanjing University of Science and Technology, 210094 Nanjing, China.
2. School of Chemistry and Molecular Engineering, Shanghai Key Laboratory of Green Chemistry and Chemical Processes, East China Normal University, Shanghai, 200062, China.
3. International Center for Materials Nanoarchitectonics (MANA), National Institute for Materials Science (NIMS), 1-1 Namiki, Tsukuba, Ibaraki 305-0044, Japan.
4. Department of Chemistry, College of Science, Hebei Agricultural University, Baoding 071001, Hebei, PR China.
5. School of Chemical Engineering & Australian Institute for Bioengineering and Nanotechnology (AIBN), The University of Queensland, Brisbane, QLD 4072, Australia.

Corresponding authors' email: TANG.Jing@nims.go.jp; wangx@njust.edu.cn; y.yamauchi@uq.edu.au

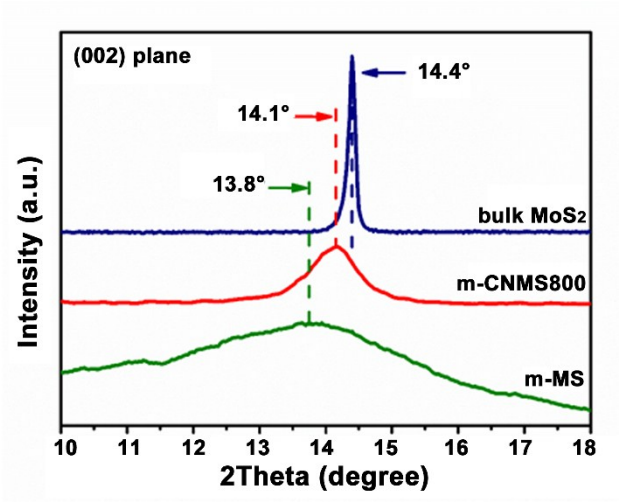

Figure S1. The selected range of XRD pattern of m-MS, m-CNMS-800 and bulk MoS_2.

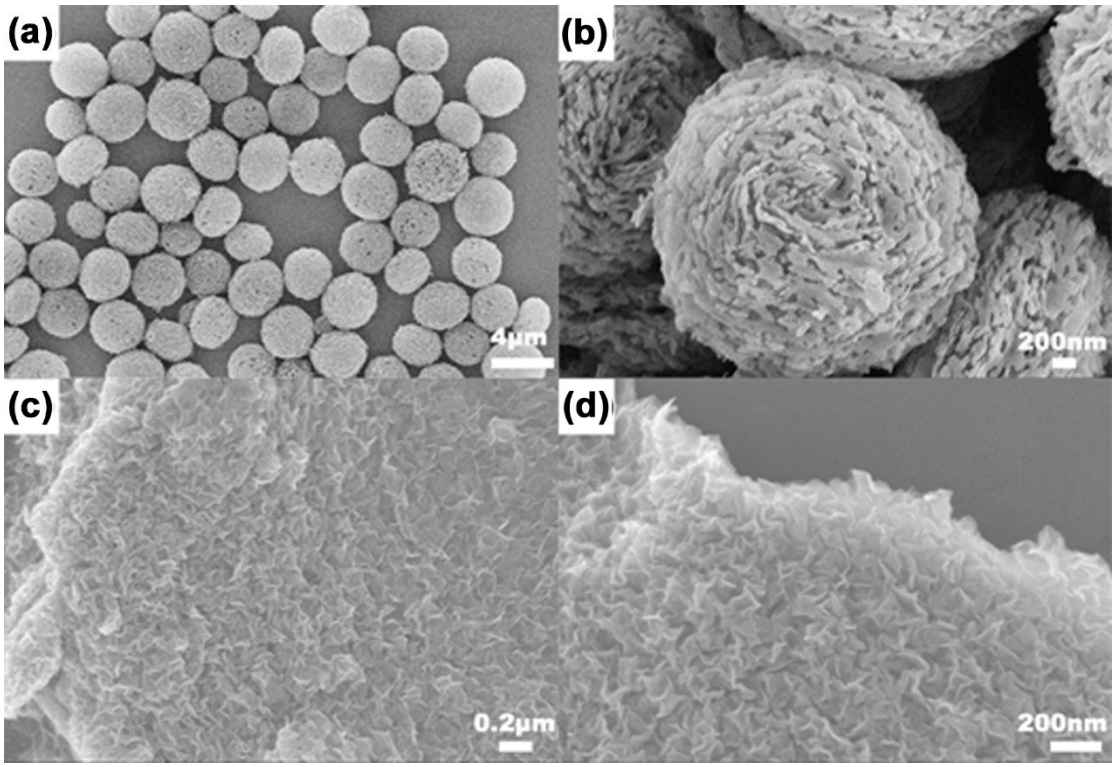

Figure S2. SEM images of (a, b) C_3N_4 template and (c, d) m-MS.

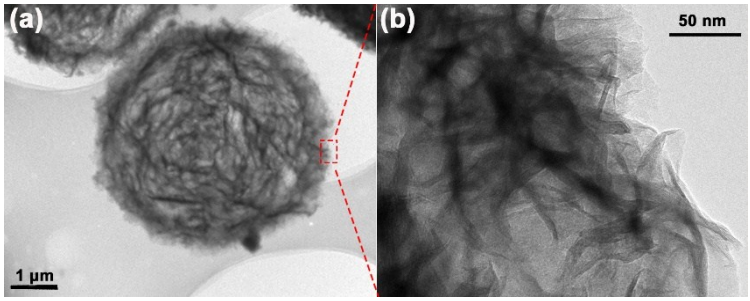

Figure S3. The TEM images of m-CNMS at a low magnification.

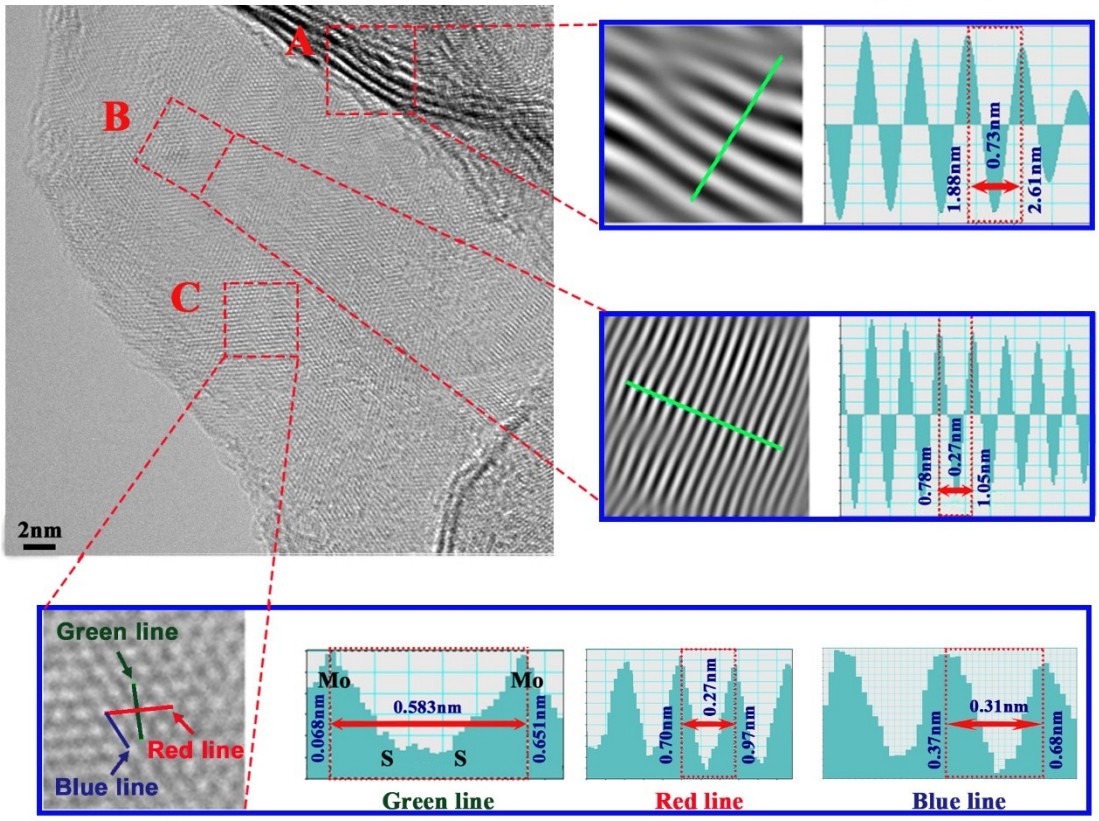

Figure S4. High-resolution TEM images of m-CNMS and the corresponding lattice distance in selected regions.

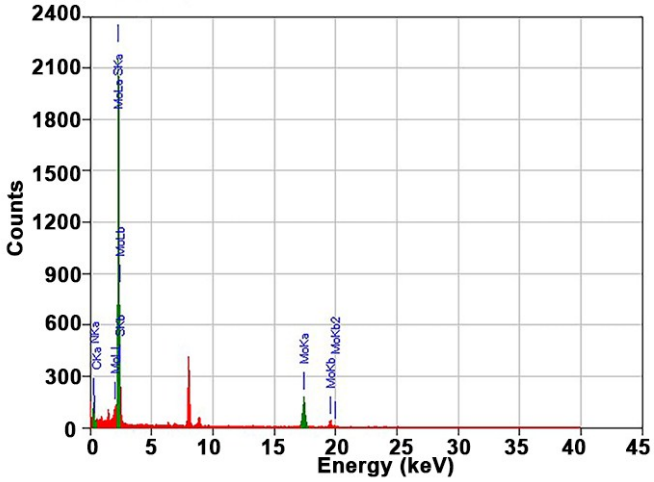

Figure S5. The EDX spectrum of m-CNMS corresponding to the EDX mapping.

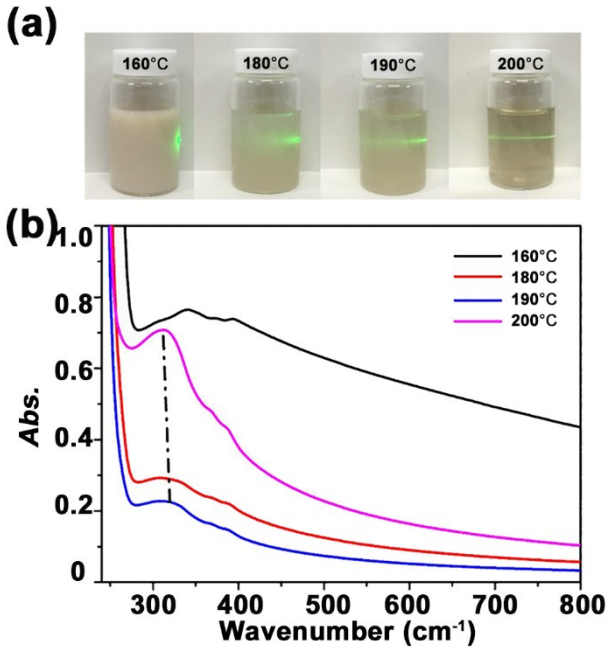

Figure S6. (a) Digital Photos of C_3N_4 after 160, 180, 190 and 200 °C hydrothermal reaction；(b) UV-Visible absorption spectra of C_3N_4 solution after different hydrothermal reaction.

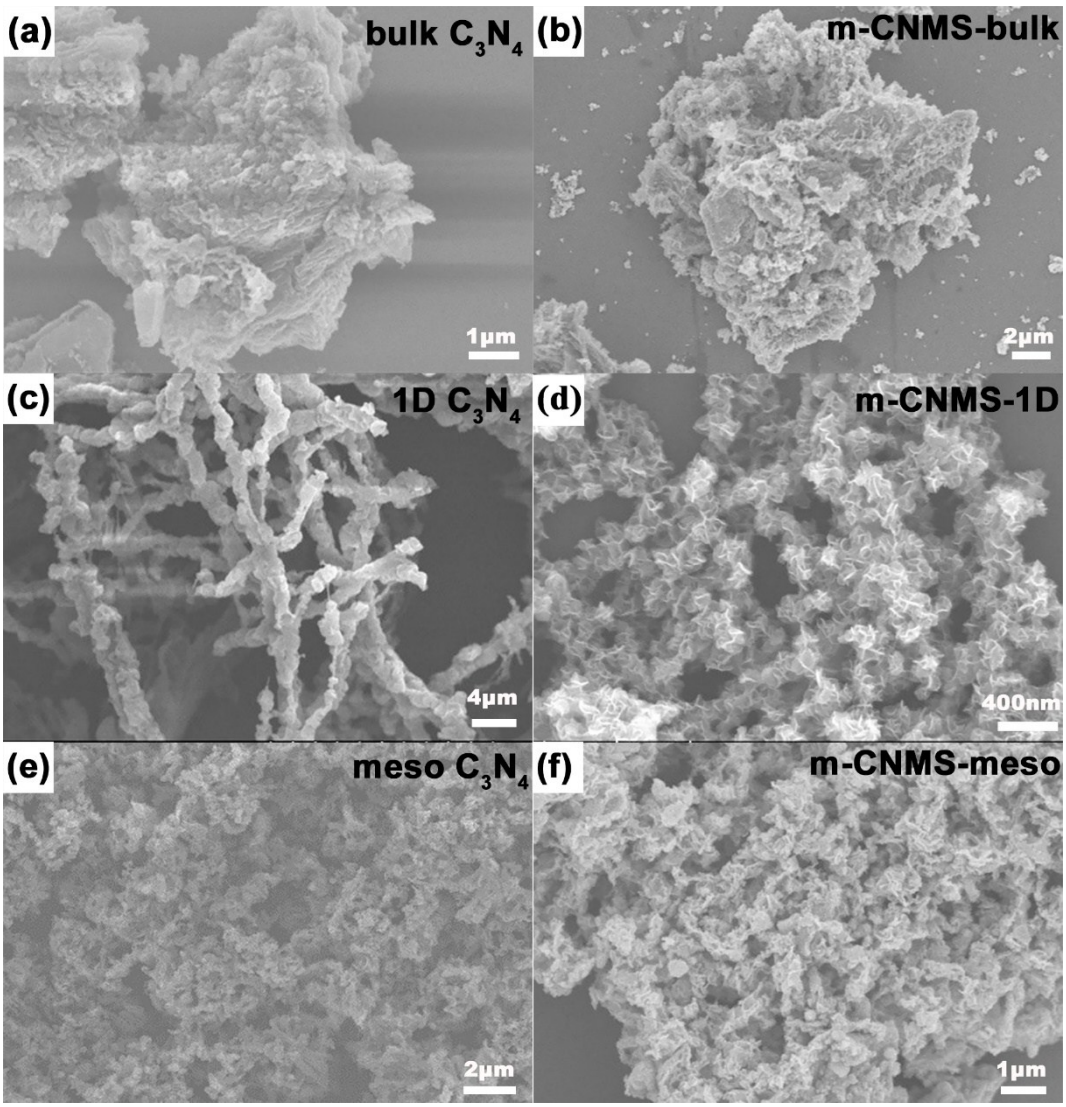

Figure S7. SEM images of C_3N_4 templates with different morphologies and the corresponding prepared MoS_2 product. Note: bulk C_3N_4 was synthesized by calcining melamine at 550 °C in air; 1D C_3N_4 was synthesized by calcining nitric acid treated melamine at 550 °C in air; meso C_3N_4 was synthesized by calcining melamine-cyanuric acid hybrid at 550 °C in air.

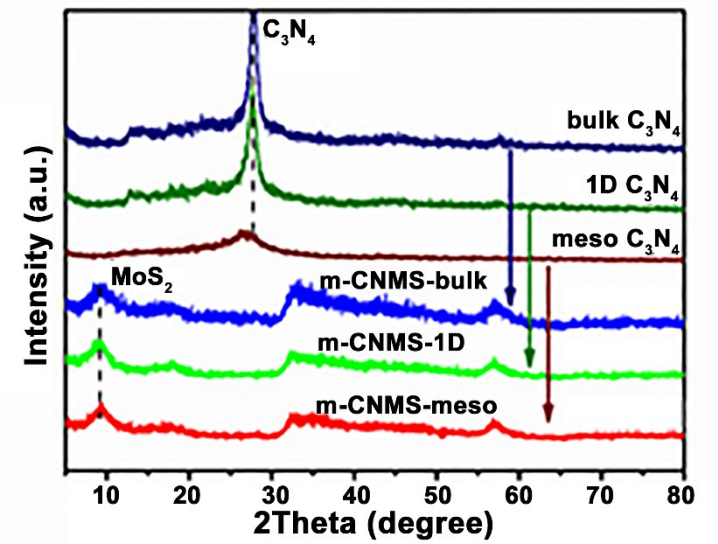

Figure S8. XRD patterns of C_3N_4 templates with different morphologies and the corresponding prepared MoS_2 product.

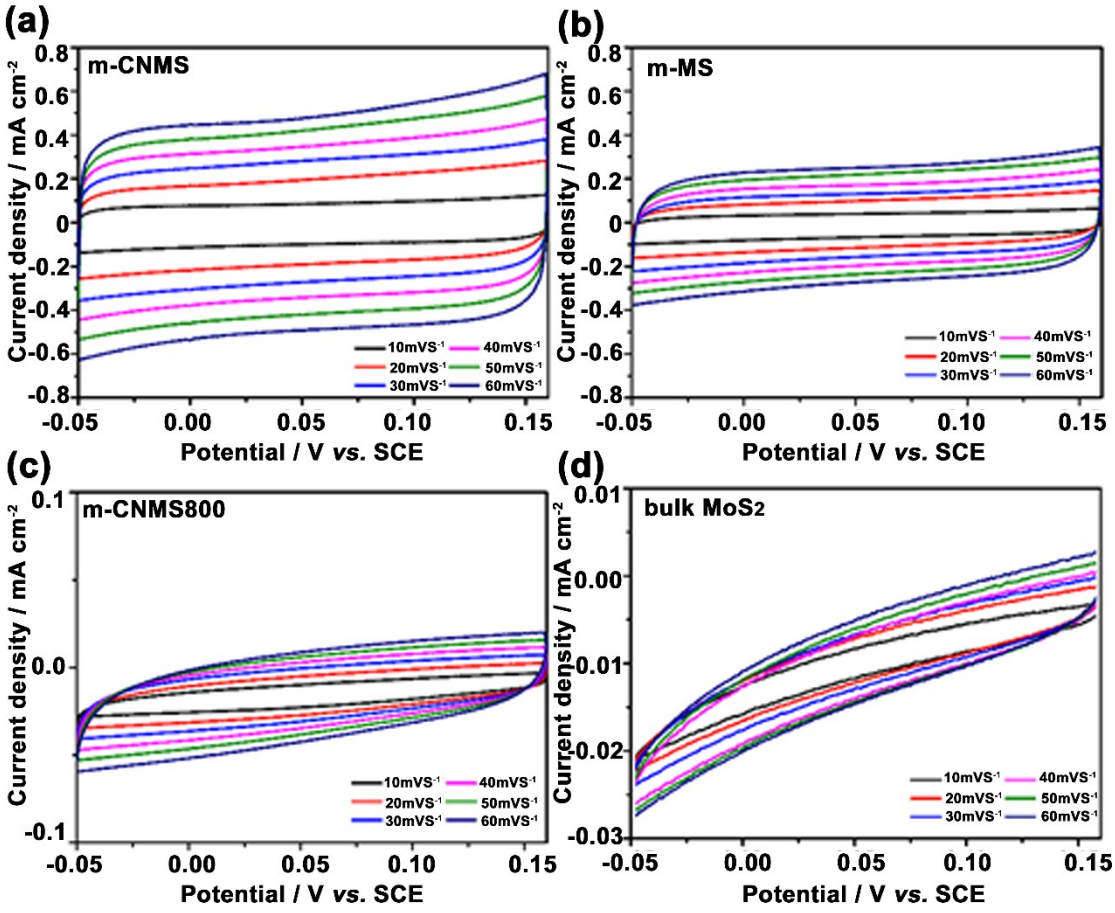

Figure S9. CV curves for m-CNMS (a), m-MS (b), m-CNMS-800 (c) and bulk MoS_2 (d). The

capacitive current of all samples was collected at 0.05 V. Note: ECSA= Cdl / Cs. Cdl is calculated by CV at various scan rates in the non-Faradaic region, and Cdl is equal to the slope of the function of double layer charging current with scan rate. Cs is a specific electrochemical double layer capacitance of an atomically smooth surface, and the value of Cs = 40 μF/cm^2 in this study.

Table S1. Element content of m-CNMS from XPS and EDX.

Element	Mo	S	C	N	S/Mo	C/N
EDX	18.5 at. %	42.6 at. %	37.4 at. %	1.5 at. %	2.3	24.9
XPS	19.2 at. %	36.9 at. %	41.6 at. %	2.3 at. %	1.9	18.0

Table S2. Comparison of HER performance of m-CNMS with other MoS_2-based electrocatalysts.

Catalysts	morphology	Current Density	Overpotential at corresponding j mA cm^{-2} (mV)	Tafel slope ($mVdec^{-1}$)	ECSA (cm^2_{ECSA})	Ref
1T MoS_2	Flower-like sphere	10 80	215 260	50.2	165	This work
1T-2H MoS_2	nanosheet	20	320	65	60.3	1.
2H MoS_2	Thin film with vertically aligned MoS_2	10	210	44	/	2.
1T' MoS_2	Nanofilm	10	175	100	/	3.
1T MoS_2	Nanosheet	10	187	43	0.55	4.
1T MoS_2	Mesoporous Nanosheet	10	153	43	1577	5.
1T MoS_2	Nanosheet	10	180	41	/	6.
2H MoS_2	Nanofilm	250	400	50	/	7.
2H MoS_2	Mesoporous foam	10	210	74	/	8.
Co_3S_4@MoS_2	Hollow ZIF-like structure	10	210	88	202.5	9.
2H-1T MoS_2	vertically aligned flakelet on nanosheet	10	203	60	/	10.

Reference

1. Wang S.; Zhang D.; Li B., Ultrastable In-Plane 1T–2H MoS_2 Heterostructures for Enhanced Hydrogen Evolution Reaction. *Adv. Energy Mater.* 2018, 8(25), 1801345.

2. Wang H.; Lu Z.; Xu S., Electrochemical Tuning of Vertically Aligned MoS_2 Nanofilms and its Application in Improving Hydrogen Evolution Reaction. *Proc. Natl. Acad. Sci.* 2013, 110(49), 19701-19706.

3. Yu Y.; Nam G. H.; He Q., High Phase-Purity 1T′-MoS_2-and 1T′-$MoSe_2$-Layered Crystals. *Nature chem.* 2018, 10(6), 638.

4. Lukowski M. A.; Daniel, A. S.; Meng, F.; Forticaux A.; Li L.; Jin S, Enhanced Hydrogen Evolution Catalysis from Chemically Exfoliated Metallic MoS_2 Nanosheets. *J. Am. Chem. Soc.* 2013, 135(28), 10274-10277.

5. Yin Y.; Han J.; Zhang Y, Contributions of Phase, Sulfur Vacancies, and Edges to the Hydrogen Evolution Reaction Catalytic Activity of Porous Molybdenum Disulfide Nanosheets, *J. Am. Chem. Soc.* 2016, 138(25), 7965-7972.

6. Geng X.; Sun W.; Wu W., Pure and Stable Metallic Phase Molybdenum Disulfide Nanosheets for Hydrogen Evolution Reaction, *Nature commun.* 2016, 7, 10672.

7. Voiry D.; Fullon R.; Yang J., The Role of Electronic Coupling between Substrate and 2D MoS_2 Nanosheets in Electrocatalytic Production of Hydrogen, *Nature Mater.* 2016, 15(9), 1003.

8. Deng J.; Li H.; Wang S., Multiscale Structural and Electronic Control of Molybdenum Disulfide Foam for Highly Efficient Hydrogen Production, *Nature commun.* 2017, 8, 14430.

9. Guo Y.; Tang J.; Qian H.; Wang Z.; Yamauchi Y, One-Pot Synthesis of Zeolitic Imidazolate Famework 67-Derived Hollow Co_3S_4@MoS_2 Heterostructures as Efficient Bifunctional Catalysts, *Chem. Mater.* 2017, 29(13), 5566-5573.

10. Yang J.; Wang K.; Zhu J.; Zhang C.; Liu T, Self-Templated Growth of Vertically Aligned 2H-1T MoS_2 for Efficient Electrocatalytic Hydrogen Evolution. ACS Appl. Mater. Inter. 2016, 8(46), 31702-31708.